J Mater Sci: Mater Med (2007) 18:435–440
DOI 10.1007/s10856-007-2002-4

# Ion implantation modified stainless steel as a substrate for hydroxyapatite deposition. Part I. Surface modification and characterization

**L. Pramatarova · E. Pecheva · V. Krastev · F. Riesz**

Received: 11 July 2005 / Accepted: 24 October 2005


**Abstract** Material surfaces play critical role in biology and medicine since most biological reactions occur on surfaces and interfaces. There are many examples showing that the surface properties of the materials control and are directly involved in biological reactions and processes in-vitro like blood compatibility, protein absorption, cell development, etc. The rules that govern the diversity of biological surface phenomenon are fundamental physical laws. Stainless steel doped with Cr, Ni and Mo is widely used material in medicine and dentistry due to its excellent corrosion resistance and mechanical properties. The interest in this material has stimulated extensive studies on improving its bone-bonding properties. This paper describes the surface modification of Cr-Ni stainless steel (AISI 316) by a whole surface sequential implantation of Ca and P ions (the basic ions of hydroxyapatite). Three groups of stainless steel samples are prepared: (i) ion-implanted, (ii) ion-implanted and thermally treated at 600°C in air for 1 h and (iii) initials. The surface chemistry and topography before and after the surface modification are characterized by X-ray photoelectron spectroscopy, Auger electron spectroscopy, magic mirror method, atomic force microscopy and contact angle measurements.

L. Pramatarova · E. Pecheva (✉)
Institute of Solid State Physics, Bulgarian Academy of Sciences, 1784 Sofia, Bulgaria
e-mail: emily@issp.bas.bg

V. Krastev
Institute of General and Inorganic Chemistry, Bulgarian Academy of Sciences, 1113 Sofia, Bulgaria

F. Riesz
Research Institute for Technical Physics and Materials Sciences, Hungarian Academy of Sciences, 1121 Budapest, Hungary

## 1 Introduction

Artificial materials used for implants in medicine and dentistry traditionally employ titanium and its alloys, as well as stainless steel because of its high fracture and corrosion resistance, easy handling and comparatively low cost.

Surface modification of biomaterials is a way widely used to improve their performance since biomaterials are intended to be exposed to a variety of aggressive body liquids. Many methods are used for surface treatment such as ion-beam sputtering [1], ion-beam assisted deposition [2, 3], plasma sputtering [4], pulsed laser ablation [5–7], self-assembled monolayers [8, 9], and etc.

On the other hand hydroxyapatite [HA, $Ca_{10}(PO_4)_6(OH)_2$] used as an artificial bone material, is one of the best biocompatible coatings for metallic protheses used inside the human body. Many approaches involve chemical modification of the surface for HA formation [10–12], sol-gel dip coating and precipitation from solution [13]. The use of nanostructures deposited onto the surface is also very promising [14, 15].

In order to tailor the surface of inorganic materials to be bioactive, a biomimetic method of coating the surface with HA is usually applied. This method involves the immersion of the material into a solution, supersaturated with respect to calcium and phosphorus, and known as simulated body fluid (SBF) [13, 16]. The composition, ion concentrations, and pH of SBF are close to those found in human blood plasma. Most of the reactions in a solution occur at the solution/solid interface. In this sense, the material surface plays an important role, because surface properties are directly related to the in-vitro biological performance such as protein adsorption and cell growth [17].

A well-known technique for chemical and topographical modification of materials is the ion implantation [18]. Its main advantage is the selective change of the surface

properties while preserving the bulk properties. In the area of biointerfaces surface modification by ion implantation is being actively employed to create surfaces with tailored biological activity by controlling their chemistry, topography, or mechanical properties. Focused ion beams are used to create nanometer-scale defects with controlled protein absorption properties [19]. For surface activation (induction of nucleation points), different ions have been implanted [20–24]. Mainly Ca and P, the basic ions of HA, were implanted simultaneously or separately [25–27]. Thus, the ion implantation appears as one of the possible techniques to induce HA formation by inducing topographical and chemical changes on the material surfaces. The thermal treatment of the ion-implanted surfaces in different ambient (in air, in oxygen atmosphere) is regarded as a mean to convert the implanted species to CaO and $P_2O_5$, hence forming surface oxide layers that will also influence the formation of calcium phosphates (CaPs) in an aqueous interfacial environment [25–27].

In this work we report the modification of AISI 316 stainless steel surface by a whole surface sequential implantation of Ca and P ions in controllable concentration, distribution, and penetration. Three groups of stainless steel samples are prepared for studying the HA growth from SBF: (i) ion implanted, (ii) ion-implanted and thermally treated at 600°C in air for 1 h and (iii) initials which are standardly polished.

## 2 Experimental details

### 2.1 Materials

Substrates with sizes of 8 mm × 8 mm × 1 mm are cut from AISI 316 stainless steel foil (Goodfellow, England; Fe 69 wt.%, Cr 18 wt.%, Ni 10 wt.%, Mo 3 wt.%, Mn < 2 wt%, C < 1200 ppm, density 7.96 g/cm$^3$). After lapping with SiC grinding papers (P320, P600 and P1000) and polishing with PA-W and G standard polishing cloths using a diamond suspension of 3 μm, the samples are ultrasonically rinsed for 3 min in alcohol and for the same time in acetone, and dried in air. Substrates prepared in this way are called initial stainless steel, and further in the text the symbol SS is used.

### 2.2 Ion implantation and theoretical calculations. Thermal treatment

Sequential implantation of Ca and P ions is conducted to modify the whole surface of initial stainless steel samples. To select appropriate parameters for the implantation, theoretical calculations are performed with a Profile Code Program (version 3.20, Implant Sciences Corporation, Wakefield, Massachusetts). Ca and P profiles into stainless steel are simulated by varying the ion energies and doses in such way that the ion distribution is in the near surface region (<100 nm), and the ion profiles are overlapped. The latter condition is theoretically and experimentally attained by implanting first the heavier Ca ion and subsequently P. In the opposite case Ca ions will push the lighter P ions deeper and the desired profile overlapping will not be obtained. The data from calculations are used for the implantation. The samples are implanted on a Danfisyk High Current Implanter (model 1090, Denmark, 200 keV) and Implanter 2 (FZR-Dresden, Germany, 10–60 keV). Applied doses, according calculations are in the range $7 \times 10^{16}$–$2 \times 10^{17}$ Ca ions/cm$^{-2}$ and $5 \times 10^{16}$–$8 \times 10^{16}$ P ions/cm$^{-2}$. To reach an approximately homogeneous distribution, the implantation is conducted using three consecutive energy steps: 104, 92, and 80 keV for Ca ions and 61, 54, and 47 keV for P ions. After ion implantation, part of the samples is thermally treated at 600°C in air for 1 h to convert Ca and P to oxides. Further in the text, the ion-implanted samples and the thermally treated samples are denoted as SS0 and SS873, respectively.

### 2.3 Analyses

The surface chemistry and topography before and after the surface modifications are studied by X-ray photoelectron spectroscopy (XPS), Auger electron spectroscopy (AES), magic mirror method (MMM), atomic force microscopy (AFM) and contact angle measurements.

XPS and AES measurements are performed on a Microlab 310 Fisons electron spectrometer to investigate the surface chemistry of SS, SS0, and SS873 samples. Mg $K_\alpha$ excitation source is used with $E = 1253.6$ eV. Calibration of the binding energy is done by setting the C 1 s line to 285 eV. Depth profiling is made by 3 keV $Ar^+$ sputtering. The total sputtered depth is measured by a Dektak 800 profilometer (VEECO, USA).

AFM scanning probe and optical microscope (DualScope C-21, DME) in tapping mode under ambient conditions is used to measure the surface roughness before and after the ion implantation.

MMM uses white light to illuminate the sample surface and the resulting image is observed on a screen behind the samples [28]. It is used to observe surface stresses resulting from preliminary treatment as sawing, polishing, and from surface modifications.

To determine the surface wettability of the studied three groups of samples, a contact angle measuring system G10/DSA10 (Kruss, Germany) and water as a probing liquid is applied.

## 3 Results and discussion

The recorded XPS O 1 s peaks have a broad contour and can be considered envelopes of underlying narrower peaks. In order to evaluate the exact contribution of the oxygen

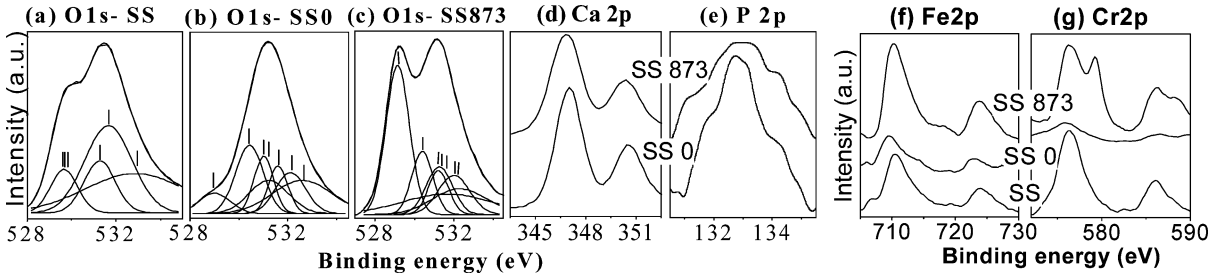


**Fig. 1** XPS spectra of stainless steel samples implanted sequentially with Ca and P ions (SS0), and the same samples treated thermally (SS873). Comparison with initial samples (SS) is carried out.

and its compounds, a peak fitting procedure is applied as shown for O 1 s in Fig. 1(a-c). Peak fitting results for SS samples (Fig. 1a) show that its surface consists of elemental oxygen (O 1 s, 531 eV), hydroxides and oxides mainly of Cr and Fe [29]. The low intensity peak at 529.8 eV is ascribed mainly to Cr-oxides ($Cr_2O_3$) because of its preferential affinity for oxygen, and also to Fe-oxides such as $Fe_2O_3$ and FeO [30, 31]. After the ion implantation compounds of the substrate elements with O, and with the implanted Ca and P, as well as compounds of Ca and/or P with O and in between themselves are additionally formed on initial samples (SS0, Fig. 1b). High surface content of $Ca_8H_2(PO_4)_6$-$5H_2O$ (OCP, 531.1 eV), $CaCO_3$ (531.2 eV), CaO (531.7 eV) and $P_2O_5$ (532.2 eV) is found by the peak fitting of O 1 s peak. Mixed oxides such as $CaCrO_4$ (529.5 eV) and $Ca_2P_2O_7$ (531.4 eV), as well as CaPs, such as $Ca_{10}(PO_4)_6(OH)_2$ (HA, 531.8 eV) and $CaHPO_4$-$2H_2O$ (DCPD, 531.5 eV) also contribute to the spectrum.

The surface of initial stainless steel is naturally covered with a native oxide layer as a result of the preliminary chemical treatment [29], confirmed also by depth profile measurements (Fig. 2a). Additionally, during the implantation of Ca and P under vacuum of about $5.10^{-6}$ mbar, residual oxygen is present in the chamber and we consider that it has been adsorbed and implanted in the samples together with the implanted species [25]. As a consequence, more than one monolayer of oxygen is always present on the sample surface, which explains the formation of so many oxygen-based compounds after the ion implantation.

The applied thermal treatment leads to an increasing signal of the metal oxides on the surface of SS873 samples (the peak at 529.8 eV in Fig. 1c) which attests the great affinity of the bombarded heated stainless steel towards oxygen [29, 32]. Peak fitting procedure allowed us to determine also a strong increase in the surface content of $CaCrO_4$, $CaCO_3$, and HA, and a decrease of CaO, $P_2O_5$, OCP, DCPD and $Ca_2P_2O_7$ content.

Peak fitting is also applied for the XP spectra of Ca 2p and P 2p (results not shown). A typical doublet of Ca 2p is observed in Fig. 1(d) [30]. The surface components that

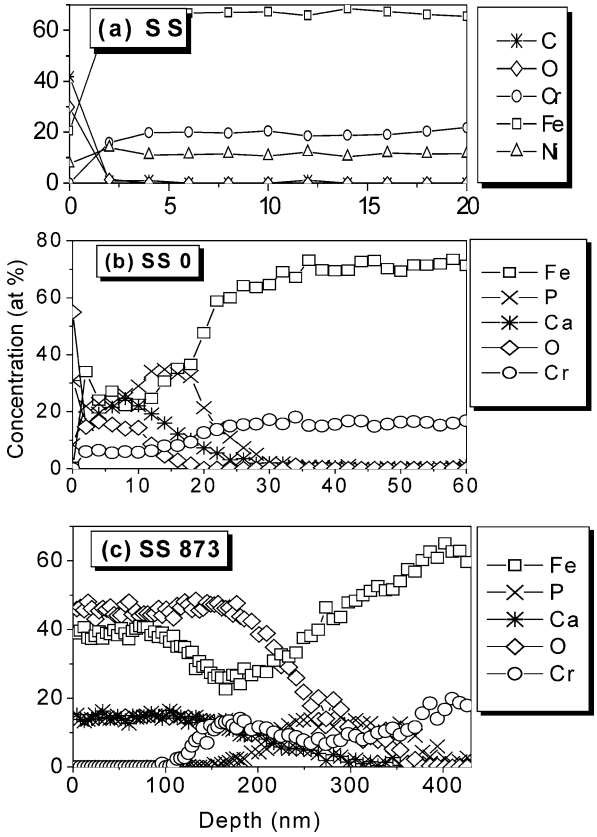


**Fig. 2** AES spectra show the elemental depth distribution in stainless steel samples: (a) initial, (b) Ca and P-implanted, (c) Ca and P-implanted and thermally treated at 600°C in air.

have contribution according to the peak fitting results for SS0 samples are: $CaCrO_4$ (346.3 eV), elemental Ca (346.7 eV), $CaCO_3$ ($2p_{3/2}$ at 347 eV and $2p_{1/2}$ at 350.5 eV), OCP (347.2 eV), CaO (347.3 eV), $Ca_2P_2O_7$ (347.6 eV), DCPD (347.8 eV) and HA (347.8 eV). The recorded on SS0 samples P 2p spectrum (Fig. 1e) is also ascribed to the CaPs discussed in the spectra of Ca 2p, and to $FePO_4$ (134.2 eV), $P_2O_5$ (134.8 eV), and $Ca_2P_2O_7$ (133.8 eV) [30, 31]. After the thermal treatment the same tendency as described for the O 1 s spectra of SS873 samples (the peak fitting results) is found for Ca 2p and P 2p.

A doublet structure is observed in the spectra of Fe 2p and Cr 2p recorded on SS, SS0 and SS873 samples (Fig. 1f, g) [30]. The peaks are ascribed to Fe and Cr in various bonding states: $Fe_2O_3$ $2p_{3/2}$ (709.9 eV), FeO (709.9 eV), also $FePO_4$ (712.8 eV) and $Fe_3C$ (708.1 eV) are present on the surfaces. A shoulder at 705.8–706.7 eV is assigned to elemental Fe (707 eV) and the second peak at 723.1–723.9 eV is typical for $Fe_2O_3$ $2p_{1/2}$. Spectra of Cr 2p correspond to $Cr_2O_3$ $2p_{3/2}$ (576.5 eV), $CaCrO_4$ (578.9 eV), and also to $Cr_2C_3$. The peak at 579.2 eV for the thermally treated samples is assigned to $CaCrO_4$ and the one at 586–586.6 eV to $Cr_2O_3$ $2p_{1/2}$ [31].

The higher doses of implantation with Ca and P ions lead to more intensive Ca, P and O peaks compared with that of Fe and Cr. This corresponds to incorporation of higher concentrations of the implanted species into the stainless steel matrix.

XPS results are supported by sputter depth profiles measured by AES (Fig. 2) which allowed us to determine the oxygen content and the thickness of the oxide layers formed as a result of the applied modifications on the surface of stainless steel. The oxygen depth distribution in the initial samples up to 2 nm (Fig. 2a, SS samples) shows the presence of a native oxide layer with a concentration of 30 at.% at the surface. AES spectrum shows that the ion implantation increases the oxygen content to 55 at.% at the very near surface as already shown by XPS. Well-defined, overlapping and narrow profiles of Ca and P with maximum relative concentrations of 25 at.% for Ca at a depth of 8 nm and 35 at.% for P at 15 nm are observed in SS0 samples (Fig. 2b). A decrease of the near surface concentrations of Fe and Cr with the implantation of Ca and P ions is also observed after the Ca and P implantation. This fact supports the conclusion for Ca and P incorporation within the stainless steel matrix and the production of surfaces depleted in Fe and Cr. AES also shows broadening of Ca and P depth profiles with the higher doses of implantation and a change of the relative concentrations to 20 at.% for Ca and 40 at.% for P.

After the thermal treatment the profiles of Ca and P (Fig. 2c, SS873 samples) are shifted from the surface (max. relative concentrations of 15 at.% for both ions at 100 and 300 nm respectively) and became diffused. Especially P penetrates deeper into the bulk of the samples. The oxide layer thickness (maximum O concentration of 45 at.%) increases up to 350 nm. Oxygen follows the Ca penetration, a reason to conclude the formation of calcium oxides. From both implanted species P is less reactive towards O since it needs four O atoms to form $PO_4$ groups, when Ca needs only one O atom to form CaO [27].

General topography of the implanted and thermally treated stainless steel samples, compared to initials (Fig. 3) is observed with MMM [28]. The image of the surfaces illuminated with white light is observed on a screen behind the samples. Combination of small light and dark areas is observed on the surfaces of steel samples with the light areas corresponding to convex surface and the dark—to concave one. These areas form surface grain structure, which could be a result of the preliminary treatment (cleaning and polishing of the surfaces) that induces surface roughness and/or a result of the ion implantation. The lines observed at the edges of the samples are due to light interference on the edges. A distortion of the samples is seen in Fig. 3(b, c) and is more significant for the implanted samples (SS0). Dark central area is observed in the image of SS873 and comes from the thicker oxide layer resulting from the thermal treatment. White round spots with size 1.5–3 mm observed in Fig. 3(b, c) are the place of $Ar^+$ ion sputtering carried out by AES measurements.

Detailed results for the topography and the average surface roughness of the implanted stainless steel samples (SS0), compared to initials (SS) are obtained with AFM (Fig. 4). Areas with sizes from 0.1 to 20 μm are scanned and the presented images are 5 × 5 μm in sizes. The measurements show that the preliminary surface treatment brings the formation of specific structure (Fig. 4a) observed also with MMM

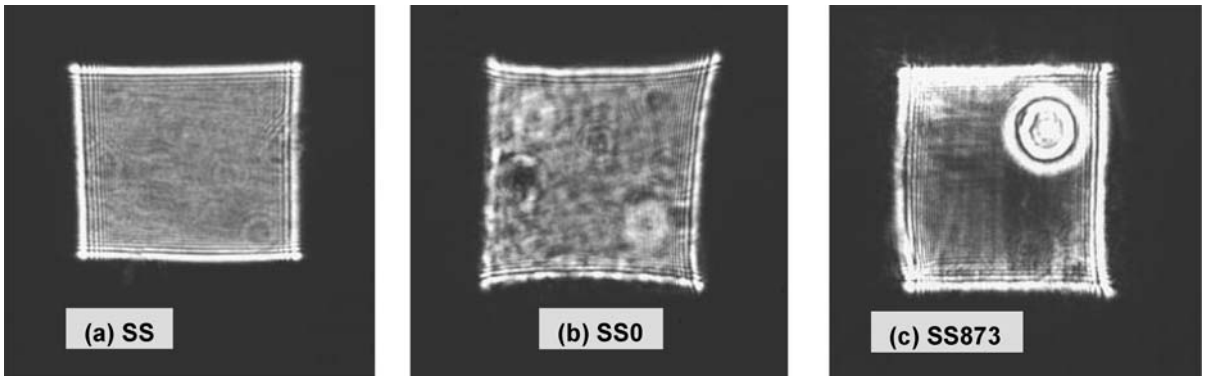


**Fig. 3** MMM method shows the general topography of stainless steel samples: (a) initial, (b) Ca and P implanted, (c) thermally treated after the implantation (samples size 8 × 8 mm).

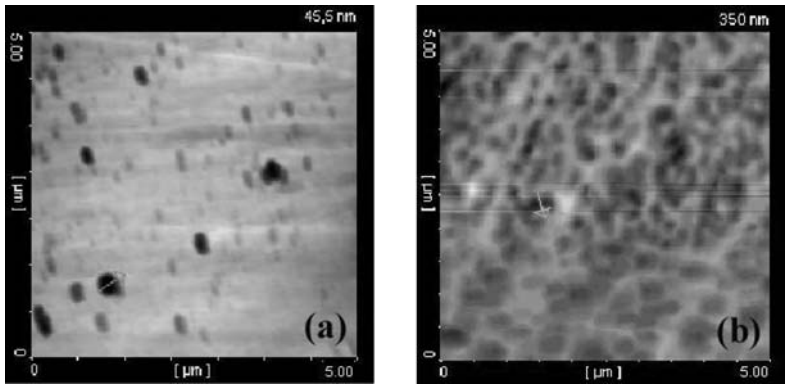


**Fig. 4** AFM show 2D topographic images of the studied samples and their average surface roughness: (a) SS, (b) SS0 samples.

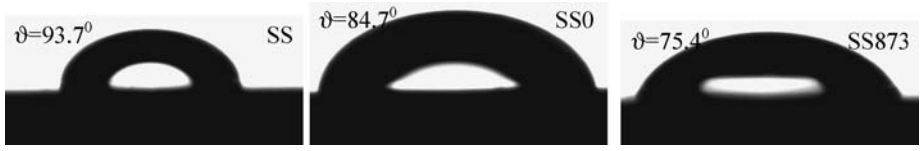


**Fig. 5** Figure showing the way in which a water drop is spreading on the modified stainless steel surfaces which illustrates their wettability.

investigation. The standard treatment induces surface roughness in the order of 45.5 nm for SS samples (the values are seen in the upper right corner of the figures). The particles observed in the SS image are probably left on its surface after the lapping and polishing of the steel surface. The ion implantation induces grain structure on the surface after the incorporation of Ca and P ions into the steel matrix (Fig. 4b). The implantation also increases the average surface roughness to 350 nm and it could be said that the surface modification by ion implantation imports changes of nanometer size in the surface topography of the material. This observation could also explain the low intensity of some XPS peaks, which is due to defocusing of the emitted electrons from the amorphized surface and decrease of the number of electrons reaching the detector.

In the case of system like "biomaterial—solution," the interactions taking place at the interface are regarded as an important factor showing the biological compatibility of the materials [33]. For that reason we investigated the wettability and the surface energy of the modified and initial surfaces before their immersion in the SBF. The results for the measured contact angle θ are presented in Table 1 and show high value for SS samples which decreases from 93.7° to 84.7° after the ion implantation (SS0 samples) and to 75.4° after the thermal treatment (SS873 samples). Since the experimental line between hydrophilic and hydrophobic surface is not strictly defined, it could be accepted that the three investigated steel surfaces are hydrophobic. We attribute the tendency of gradually decrease of θ of the initial sample in direction to the thermally treated steel sample to the increase of the oxide layer thickness [34]. The way in which a water drop is spreading on the different surfaces is shown in Fig. 5 and illustrates their wettability. The surface energy is also a measure for the wettability of the surfaces and has the following dependence on θ: high contact angle means low surface energy, and the opposite. Since biomaterials are in continuous contact with biological fluids that are generally aqueous, it has to be mentioned that a well wettable surface is expected to facilitate the adhesion of biological layers and to increase their resistance to be detached off the surface. It is known also that wettable steel surface has higher corrosion resistance. In order to study the influence of the two types of modification of the stainless steel on the HA nucleation and layer growth, a biomimetic approach is applied [35], i.e. immersion of the samples in a supersaturated SBF at physiological conditions (37°C and pH 7.4).

**Table 1** The results from the measurement of the contact angle θ between a water drop and the surfaces of ion implanted and thermally treated stainless steel samples compared to initials

| Samples | θ (°) | Surface energy (mN/m) |
|---|---|---|
| SS | 93.7 ± 0.3 | 35.26 |
| SS0 | 84.7 ± 0.3 | 33.88 |
| SS873 | 75.4 ± 0.4 | 32.05 |

## 4 Conclusions

Following sequential implantation of Ca and P ions, chemical and topographical modification of AISI 316 stainless steel surface is attained. Peak fitting of the recorded XP spectra shows the formation of Ca and P-based compounds, such as HA, dicalcium phosphate dihydrate and octacalcium phosphate, CaO, $CaCO_3$, $Ca_2P_2O_7$, $P_2O_5$, as well as predominant oxides of Cr and Fe. The applied subsequent thermal treatment in air leads to an increasing signal of the metal oxides on the surface and also to a strong increase in the surface content

of $CaCrO_4$, $CaCO_3$, and HA, and a decrease of CaO, $P_2O_5$, octacalcium phosphate, dicalcium phosphate dihydrate and $Ca_2P_2O_7$ content. The higher doses of implantation leads to a thicker layer of Ca and P-containing oxides (Ca oxides predominate), as well as to the formation of CaP precursors expected to facilitate the HA formation in a supersaturated SBF. The results from the AES reveal the presence of a native oxide layer on the surface of initial stainless steel samples, which increases after the ion implantation, and especially after the thermal treatment of the surfaces.

AFM study shows that the ion implantation yields the formation of surface grain structure in the stainless steel and nanometer-sized surface roughness (45.5 nm before and 350 nm after the implantation). The decrease of the contact angle of the initial samples after the implantation and the thermal treatment yields a conclusion for dependence of the surface wettability on the increasing thickness of the surface oxide layer.

**Acknowledgments** We would like to thank our colleagues Dr. M. F. Maitz, Dr. M. T. Pham, as well as I. Winkler, G. Winkler and Dr. Richter for the ion implantation, E. Quaritsch and Dr. H. Reuther for XPS/AES measurements, Dr. Ch. Bilke-Krause for contact angle measurements. This research was supported by a Marie Curie grant No HPMT-CT-2000-00182 of the European Community and in part, by the Bulgarian National Scientific Research Fund through Grant L1213/2002. The Hungarian part was supported, in part, by grants OTKA T 037711, OTKA M 041735 and GVOP-3.2.1.-2004-04-0337/3.0.

## References

1. J. ONG, L. LUCAS, W. LACEFIELD and E. RIGNEY, *Biomaterials* **13 (4)** (1992) 249.
2. A. EKTESSABI, *Nucl. Instr. Methods Phys. Res. B* **127/128** (1997) 1008.
3. J. LIU, Z. LUO, F. CUI, X. DUAN and L. -M. PENG, *J. Biomed. Mater. Res*. **52** (2000) 115.
4. W.-J. LO, D. GRANT, M. BALL, B. WELSH, S. HOWDLE, E. ANTONOV, V. BAGRATASHVILI and V. POPOV, *J. Biomed. Mater. Res*. **50** (2000) 536.
5. J. ARIAS, M. MAYOR, J. POU, B. KEON and M. PEREZ-AMOR, *Appl. Surf. Sci.* **434** (2000) 154–155.
6. M. BALL, S. DOWNES, C. SCOTCHFORD, E. ANTONOV, V. BAGRATASHVILI, V. POPOV, W.-J. LO, D. GRANT and S. HOWDLE, *Biomaterials* **22** (2001) 337.
7. L. CLERIES, J. FERNANDEZ- PRADAS and J. MORENZA, *Biomaterials* **21** (2000) 1861.
8. J. AIZENBERG, *J. Crys. Growth* **211** (2000) 143.
9. A. CAMPBELL, G. FRYXELL, G. GRAFF, P. RIEKE and B. TARASEVICH, *Scan. Microsc.* **7(1)** (1993) 423.
10. H. WEN, Q. LIU, J. WIJN, K. DE GROOT and F. CUI, *J. Mater. Sci.: Mater. Med*. **9** (1998) 121.
11. T. KOKUBO, F. MIYAJI, H. KIM and T. NAKAMURA, *J. Am. Chem. Soc.* **79** (1996) 1127.
12. H. KIM, F. MIYAJI, T. KOKUBO, S. NISHIGUCHI and T. NAKAMURA, *J. Biomed. Mater. Res*. **45** (1999) 100.
13. T. KOKUBO, H. KUSHITANI, S. SAKKA, T. KITSUGI and T. YAMAMURO, *J. Biomed. Mater. Res*. **24** (1990) 721.
14. S. BAYLISS, L. BUCKBERRY, P. HARRIS and C. ROUSSEAU, *Thin Solid Films* **297** (1997) 308.
15. L. PRAMATAROVA, E. PECHEVA, D. NESHEVA, Z. LEVI, Z. ANEVA, R. PRAMATAROVA, U. BISMAYER and T. PETROV, *Phys. Stat. Sol. C* **3** (2003) 1070.
16. M. TANAHASHI, T. KOKUBO and T. NAKAMURA, *Biomaterials* **17** (1996) 47.
17. D. CASTNER and B. RATNER, *Surf. Sci*. **500** (2002) 28.
18. P. SIOSHANSI, *Nucl. Instrum. Meth. Phys. Res. B* **767** (1987) 24–25.
19. L. HANLEY and S. SINNOTT, *Surf. Sci.* **500** (2002) 500.
20. P. EVANS, T. VILAITHONG, L. YU, O. MONTEIRO, K. YU and I. BROWN, *Nucl. Instrum. Meth. Phys. Res. B* **168** (2000) 53.
21. T. HANAWA, K. MURAKAMI and S. KIHARA, in "Characterisation and Performance of Calcium Phosphate Coatings for Implants," ASTMSTP 1196, ed. E. HOROWITZ and J. PARR, (American Society for Testing and Materials, Philadelphia, 1994) P. 170.
22. T. HANAWA, H. UKAI, K. MURAKAMI and K. ASAOKA, *Mater. Trans.*, *JIM* **36** (1995) 438.
23. M. T. PHAM, W. MATZ, H. REUTHER, E. RICHTER and G. STEINER, *J. Mater. Sci. Lett.* **19** (2000) 1029.
24. M. PHAM, M. MAITZ, W. MATZ, H. REUTHER, E. RICHTER and G. STEINER, *Thin Solid Films* **379** (2000) 50.
25. E. WIESER, I. TZYGANOV, W. MATZ, H. REUTHER, S. OSWALD, M. T. PHAM and E. RICHTER, *Surf. Coat. Technol.* **111** (1999) 103.
26. M. T. PHAM, W. MATZ, H. REUTHER, E. RICHTER, G. STEINER and S. OSWALD, *Surf. Coat. Technol.* **313** (2000) 128–129.
27. M. T. PHAM, H. REUTHER, W. MATZ and R. MUELLER, *J. Mater. Sci.: Mater. Med.* **11** (2000) 383.
28. F. RIESZ, *J. Phys. D: Appl. Phys.* **33** (2000) 3033.
29. D. STOYCHEV, P. STEFANOV, D. NICOLOVA, I. VALOV and T. S. MARINOVA, *Mater. Chem. Phys.* **73** (2002) 252.
30. C. WAGNER, W. RIGGS, L. DAVIS, J. MOULDER and G. MUILENBERG, Handbook of X-ray photoelectron spectroscopy, Perkin-Elmer Corporation, Physical Electronics Division, Eden Prairie, Minn. 55344, 1979.
31. J. MOULDER, W. STICKLE, P. SOBOL and K. BOMBEN, Reference book of standard spectra for identification and interpretation of XPS data, ed. by J. CHASTAIN and R. KING JR., Physical Electronics Division, Minn. 55344, 1979.
32. G. LUZZI and L. PAPAGNO, *J. Nucl. Mater.* **614** (1978) 76–77.
33. D. WILLIAMS, *J. Biomed. Eng.* **11** (1989) 185.
34. C. DAHMEN, A. JANOTTA, D. DIMOVA-MALINOVSKA, S. MARX, B. JESCHKE, B. NIES, H. KESSLER and M. STUTZMANN, *Thin Solid Films* **427** (2003) 201.
35. L. PRAMATAROVA, E. PECHEVA and V. KRASTEV, *J. Mater. Sci.: Mater. Med.* **X** (2005) XXX.